Academic Journal of Science and Technology
ISSN: 2771-3032 | Vol. 4, No. 3, 2022

Flow Field Simulation Analysis of Medium-Pressure Cyclone

Yilong Wang, Liang Zhang, Yangjun Qiu

School of Electrical and Mechanical Engineering, Southwest Petroleum University, Chengdu 610500, China

Abstract: Based on computational fluid dynamics (CFD) method, FLUENT software was used to analyze the flow field of the three-phase cyclone separator at medium pressure. Through the numerical simulation of the de-sanding efficiency of the cyclone, the flow field characteristics and separation efficiency of the cyclone were studied under this working condition, which provided a reference for the analysis of the cyclone under this working condition.

Keywords: Cyclone separation, Efficiency, Numerical simulation.

1. Introduction

After sand fracturing is used in shale gas exploitation, the wellhead pressure is high and the formation sand is produced more in the initial stage of drainage[1-3]. These solid particles are carried out by high-speed wellbore fluid, which will cause serious erosion and blockage of surface testing equipment, pipelines, and instruments, posing a serious threat to the safety of oil and gas well testing[4-6]. Therefore, efficient separation of solid impurities in frac flowback fluid has become the primary goal after successful recovery.

Improving the separation efficiency and reducing the energy loss of a cyclone are important issues in the theoretical research of cyclone technology[7-10]. In recent years, researchers are more inclined to CFD numerical simulation method to optimize the structure of cyclone so that it can meet the requirements of special working conditions, but most of them are limited to gas-solid or liquid-solid two-phase numerical simulation analysis[11]. In this paper, the gas-liquid-solid three-phase numerical simulation of cyclone separator was carried out by Mixture model of multiphase flow[12], and the flow field characteristics and separation efficiency under special working conditions were determined.

2. Model

2.1. Physical model

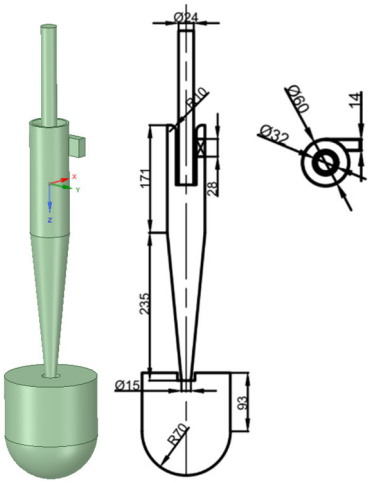

Figure 1. 3D model and structure diagram of cyclone

2.2. Mathematical model

According to the mass conservation equation of fluid dynamics, the mass inflow of fluid element in unit time is equal to the increase of mass flow of fluid element. From the mass equation of fluid dynamics, the continuum equation observed by fluid motion can be obtained:

$$\frac{\partial \rho}{\partial t}+\frac{\partial}{\partial x_j}\left(\rho u_j\right)=S_m \tag{1}$$

Among them, S_m -Mass source term,The velocity of u_j is the component in the direction of j , and the subscript 1,2 and 3 respectively represent the spatial coordinates of x, y, z . ρ - Fluid density.

The resultant force on a fluid cell is equal to the rate of change of momentum of the fluid cell with time. Momentum conservation equations in all directions can be obtained from the law of momentum conservation.

The general formula for viscous incompressible fluid is:

$$\frac{\partial\left(\rho u_i\right)}{\partial t}+\frac{\partial}{\partial x_j}\left(\rho u_i u_j\right)=-\frac{\partial p}{\partial x_i}+\frac{\partial}{\partial x_j}\left(\mu_t \frac{\partial u_i}{\partial x_j}\right)+\left(\rho-\rho_a\right) g_j \tag{2}$$

According to the first law of thermodynamics, the net heat flow into the fluid cell plus the work done by the force on the cell is equal to the rate of energy increase in the cell. The energy conservation equation is derived from the energy equation

$$\frac{\partial(\rho T)}{\partial t}+\frac{\partial}{\partial x_j}\left(\rho u_j T\right)=\frac{1}{C_p} \frac{\partial}{\partial x_j}\left(k_t \frac{\partial T}{\partial x_j}\right)+\frac{C_{\rho v}-C_{Pa}}{C_p}\left[\frac{\partial}{\partial x_j}\left(\frac{\mu_t}{\sigma_c}\right) \frac{\partial \omega}{\partial x_i}\right] \frac{\partial T}{\partial x_j} \tag{3}$$

In the energy conservation equation: k_t -Thermal conductivity of turbulent flow, the cyclone ignores the effect of temperature, which can be ignored.

2.3. Boundary condition

Combined with actual working conditions and relevant operating parameters, each boundary condition is defined as follows:

(1) Entrance conditions: The entrance is set as the speed entrance. The inlet velocity is converted to the inlet flow of

6×104m3/d, the hydraulic diameter is 18.7mm, and the liquid volume fraction is 1.55%.

(2) Outlet conditions: The outlet is set as the pressure outlet, the outlet pressure is 6.0MPa, and the outlet hydraulic diameter is set as 24mm.

(3) Wall condition: The non-slip wall condition is adopted, and the wall function approximation is applied to the wall mesh points.

(4) Physical property parameter setting: gas phase density is 57.85kg/m3, viscosity is 1.27×10-5Pa.s. The secondary phase is water and sand, and the density of fracturing sand is 1700kg/m3. In this study, a total of 1900 particles were shot, and the sand particle sizes were 75μm, 96μm, 120μm, 180μm, and 250μm, respectively. The number of particles of each particle size was equal.

3. Results and Discussion Results and discussion

In order to study the flow field distribution at different positions in the cyclone, different sections were taken from different parts of the inlet section, the cylindrical section and the cone section.

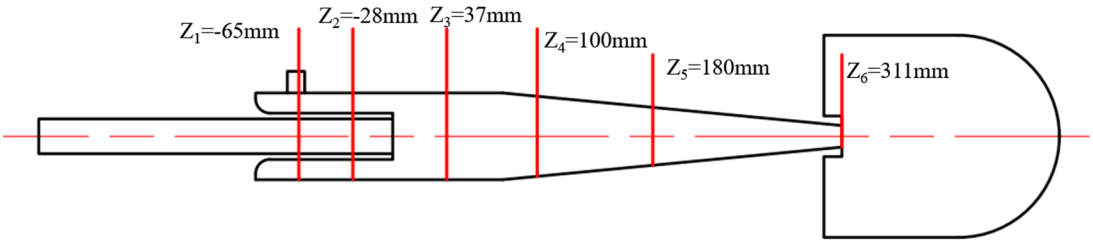

Figure 2. Selection of different sections

Figure 2 shows six diagrams of different sections. z1=-65mm is located at the entrance section; z2=-28mm located in the middle of the cylinder; z3=37mm located in the lower section of the cylinder; z4=100mm located at the upper end of the cone section; z5=180mm located in the middle of the cone section; z6=311mm is the bottom orifice

During the operation of the cyclone, the mixture of gas-water-sand enters the cyclone from the inlet pipe along the tangential direction under the action of the power source. With the energy loss, the existence of pressure gradient, centrifugal force and Stokes resistance, the mixture has radial displacement and achieves the effect of liquid-solid separation. The energy loss of the cyclone includes the jet resistance entering the device, the resistance of the material in the cyclone, the friction resistance between the material and the wall, and the kinetic energy loss of the outlet material, etc. Macroscopically, the resistance loss is mainly manifested as the pressure difference between inlet and outlet. Therefore, the study of pressure and pressure drop inside the cyclone is of great significance to the influence of separation efficiency and energy consumption of the cyclone, so the flow field pressure and internal pressure of the cyclone are studied in depth.

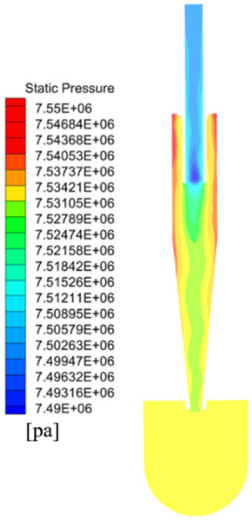

Figure 3. Pressure distribution at X=0mm

Inside the cyclone, the pressure distribution at X=0mm section is shown in Figure 3. As can be seen from the figure, the pressure is roughly distributed symmetrically. In the radial direction, the pressure gradually decreases from the wall to the central position. In the middle position, there is a cylindrical negative pressure area, with high pressure on both sides and low pressure in the middle.

FIG. 4 shows the pressure distribution cloud diagram of Z1-Z6 section. It can be seen from FIG. 4 that the pressure distribution presents asymmetry in the column section and gradually increases along the axial direction. There is a negative pressure zone in the center of the cyclone, and the pressure in the middle is lower than the pressure on both sides.

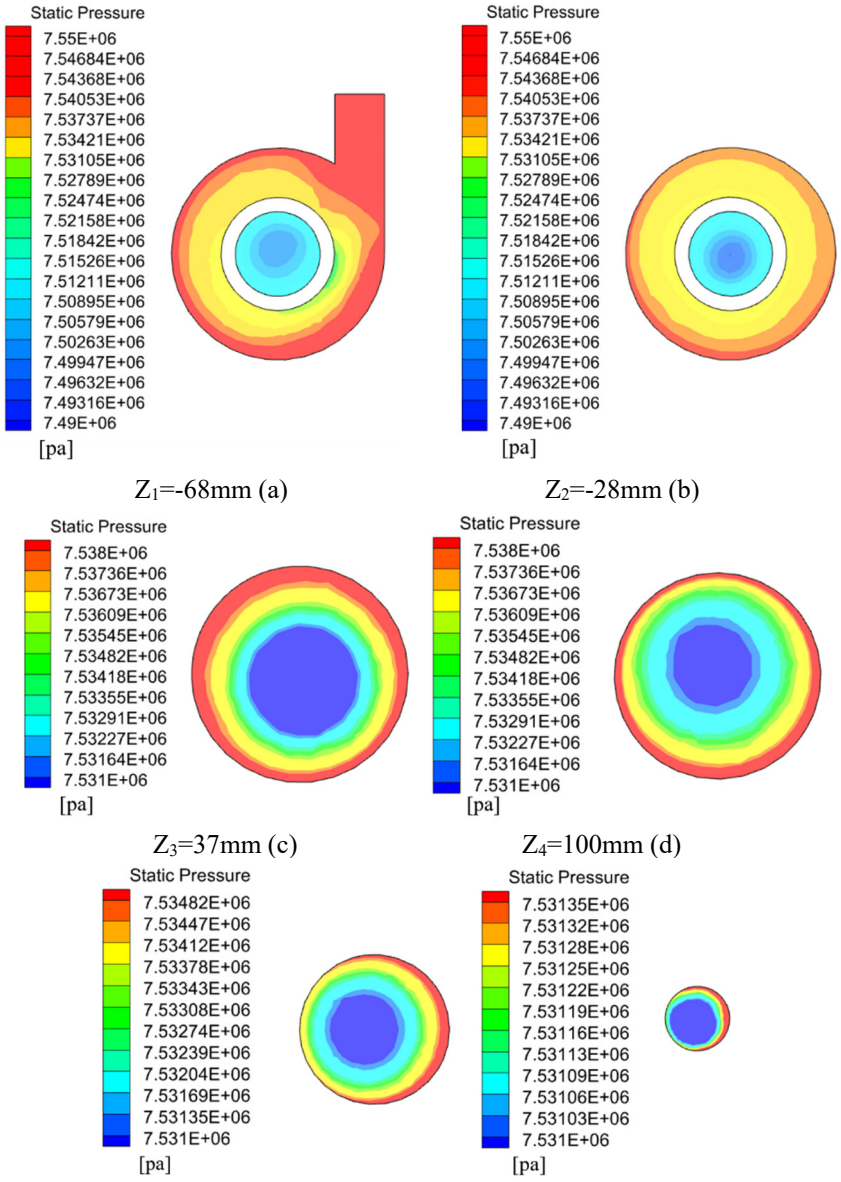

Z_1=-68mm (a) Z_2=-28mm (b)

Z_3=37mm (c) Z_4=100mm (d)

Z_5=180mm (e) Z_6=311mm (f)

Figure 4. Cross section cloud image of pressure at z1-z6

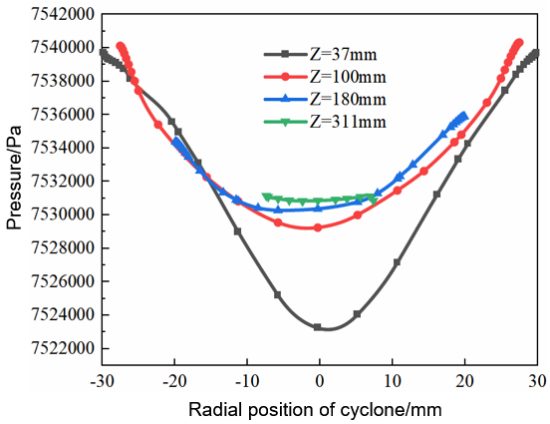

Figure 5. Internal pressure distribution

FIG. 5 shows the pressure distribution curve in the radial direction of the section. As can be seen from the figure, on the same section, from the wall of the cyclone to the central position, the pressure gradually decreases, and the pressure gradient is large, and a negative pressure region is formed in the central position. Along the axis, as the diameter decreases gradually, the energy loss between the fluid and the wall increases, so the pressure in the cone section near the wall is lower than that in the column section. From the column section to the cone section, the pressure in the central position gradually increases and does not change much at the dust outlet. This is because at the dust outlet, the contact area

between the fluid and the sediment tank changes, and the pressure at the dust outlet is gentle, which also confirms the direction of the air in the air column.

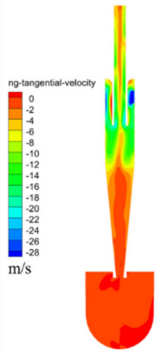

Figure 6. Tangential velocity distribution cloud map at X=0mm

In hydrocyclone, the centrifugal inertial force field is generated by tangential velocity. In the process design and development of hydrocyclone, most of the design indexes basically involve tangential velocity. Tangential velocity plays an important role in hydrocyclone, so the study of tangential velocity size and distribution provides an important basis for the research, development and design of flow field of hydrocyclone.

The figure 7 shows tangential cloud image of the cyclone X=0mm section. As can be seen from the figure above, tangential velocity increases first and then decreases from the inner wall of the cyclone to the central position. It can be clearly seen from tangential velocity cloud images of different sections in the figure. The tangential velocity below the cone section of the cyclone decreases obviously, mainly because the space of the sediment tank changes from centrifugal settlement to gravity settlement, and the closed space reduces the air fluidity.

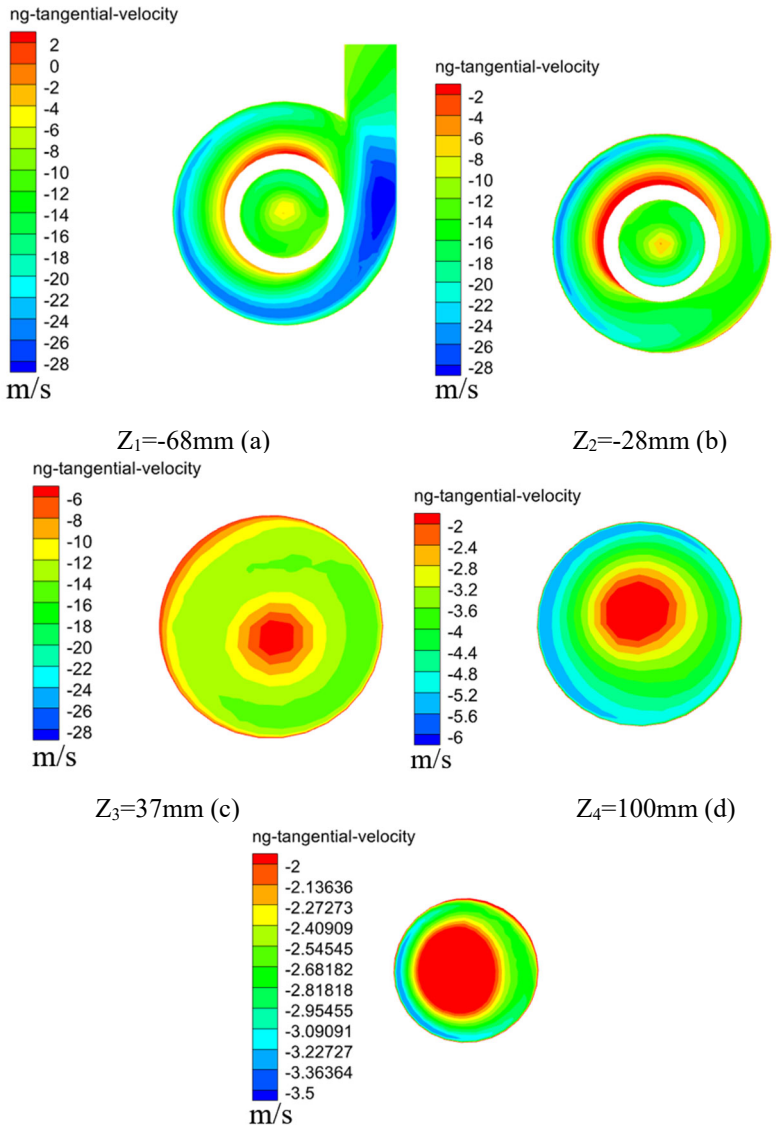

Z_1=-68mm (a)

Z_2=-28mm (b)

Z_3=37mm (c)

Z_4=100mm (d)

Z_5=180mm (e)

Figure 7. Tangential velocity cloud images of different sections

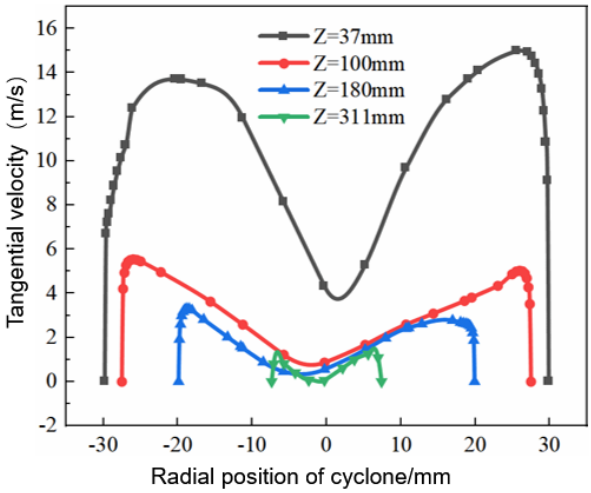

Figure 8. Tangential velocity distribution of different sections

As shown in FIG. 8, the tangential velocity inside the cyclone is humped. The tangential velocity is 0 at the wall surface. With the increase of the radius, the velocity first increases gradually, and then decreases gradually after reaching the maximum tangential velocity. From the column segment to the cone segment, the tangential velocity decreases gradually and the tangential velocity of the column segment is much larger than that of the cone segment. The distribution symmetry of tangential velocity inside the cyclone is poor. The main reason is that the single tangential inlet feed will make the cyclone feed uneven and affect the distribution of internal flow field under high pressure and large flow.

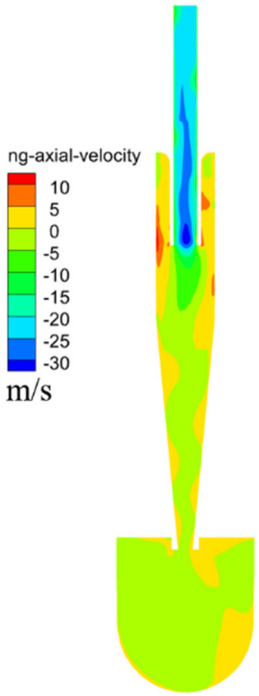

Figure 9. Axial velocity cloud map of X=0mm section

The distribution of axial velocity of a cyclone affects the distribution of the overflow port and the bottom port in the turbulent flow. From the point of view of axial velocity tangential velocity depends on the three-dimensional velocity of inlet fluid as well as axial velocity. The axial velocity mainly shows the motion of the fluid inside the cyclone desander, and its value determines the residence time of the particles inside the cyclone desander, which has a great influence on the separation accuracy of solid particles. From the distribution, the axial velocity depends on the geometry of the cyclone, especially the diameter of the overflow port, the bottom port and the cone Angle of the cyclone.

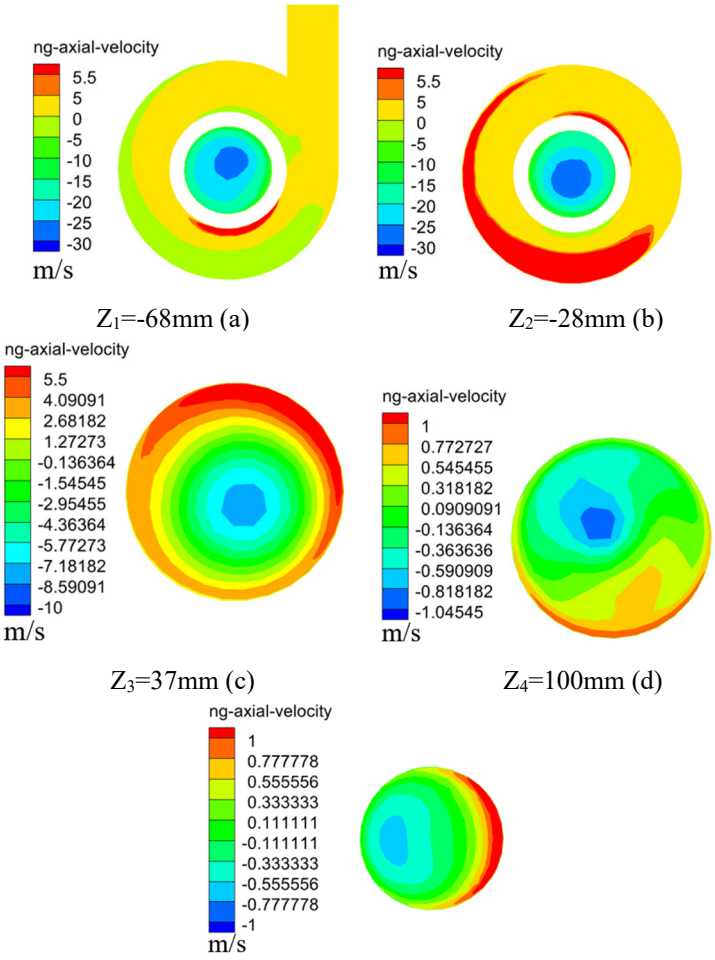

Z_1=-68mm (a) Z_2=-28mm (b)

Z_3=37mm (c) Z_4=100mm (d)

Z_5=180mm (e)

Figure 10. Axial velocity cloud images of different sections

The distribution cloud diagram of axial velocity of each section of the cyclone is shown in the figure 10. It can be seen from the figure that the axial velocity is divided into two parts: the internal cyclone moving up along the air column and the external cyclone moving down along the wall surface. The different rotation centers of different sections indicate that the distribution of flow field inside the cyclone is asymmetrical and the axial velocity decreases gradually at the bottom of the cyclone

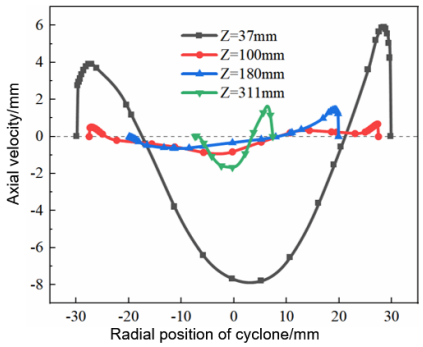

Figure 11. Axial velocity distribution of different sections

As can be seen from FIG. 11, from the wall surface to the center of the cyclone, the axial velocity increases first and then decreases, and the overall trend is consistent with the tangential velocity. However, the axial velocity difference between the column section and the cone section is large. The smaller axial velocity of the cone section can make the particles better stay in the sediment tank, reduce the fluidity of the particles moving with the fluid, and ensure that the particles can fully do centrifugal movement to improve the separation accuracy.

The intensity and distribution of turbulence will greatly affect the performance and separation efficiency of the cyclone. On the one hand, the turbulence intensity affects the energy loss of the cyclone, on the other hand, it also affects the particle phase distribution. Therefore, it is of great significance to study the turbulence intensity distribution inside the cyclone.

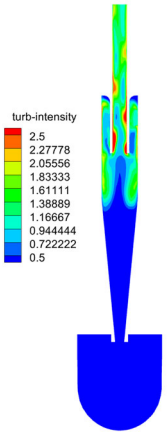

Figure 12. Cloud map of turbulence intensity at X=0mm section

FIG. 12 shows the distribution cloud diagram of turbulence intensity at X=0mm section of the cyclone. The relative turbulence in the separator can be clearly reflected through the cloud image. It can be seen from the above figure that the turbulence intensity cloud map presents a symmetrical distribution. The turbulence intensity at the upper overflow port is the most intense, gradually extends downward and decreases, and the turbulence intensity at the middle part is the lowest. Since the inlet is the place where tangential motion of the fluid begins, the turbulence intensity at the inlet is very high and the tangential velocity is very high. In addition, due to the high-speed rotation of the fluid and the wall friction, resulting in the wall turbulence intensity is also very large.

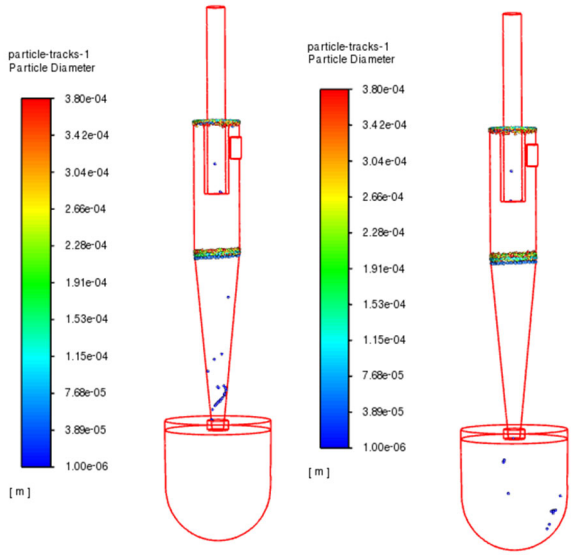

0.35s 2.35s

Figure 13. Particle distribution at different times

FIG. 13 shows the particle distribution at different times. It can be seen from the figure that as time goes by, particles move spirally down along the pipe wall from the dust outlet to the dust chamber and settle. Under this condition, the separation efficiency of the cyclone is 90.62%, achieving the separation effect.

4. Summary

(1) On the same section, from the wall of the cyclone to the central position, the pressure decreases gradually, and the pressure gradient is large, and the negative pressure area is formed in the central position.

(2) The tangential velocity below the cone section of the cyclone decreases significantly, mainly because the space of the sediment tank changes from centrifugal settlement to gravitational settlement, and the closed space reduces the air fluidity.

(3) The turbulence intensity at the upper overflow port is the most intense, and gradually extends downward and decreases, while the turbulence intensity at the middle part is the lowest.

References

[1] Wang Shuli, Wang Lei, Cui Baoyu, et al. Effect of flat bottom structure on flow field characteristics and separation performance of hydrocyclone [J]. Nonferrous Metals (Mineral Processing Section),2022(06):141-146.

[2] Duan Xiaoyao, Zhang Debao, Zhang Fan, et al. Influence of cyclone intensity on Flow Field of three-stage Miter Cyclone [J]. Turbine Technology,202,64(03):187-190+194.

[3] Cui Baoyu, Ma Congyu, Shen Yanbai, et al. Design of Inlet Diameter of Hydrocyclone Based on Steady Flow Field [J]. Journal of Northeastern University (Natural Science), 2021, 42(07): 1005-1011.

[4] Li Feng, Liu Peikun, Yang Xinghua, et al. Numerical Simulation of Effect of Rectangular Feed Body Aspect Ratio on Flow Field and Separation Performance of Cyclone [J]. Fluid Machinery, 201,49(02):43-50. (in Chinese)

[5] Li Feng, Liu Peikun, Yang Xinghua, et al. Numerical Simulation of Flow Field in a Gradual Exit Cyclone [J]. Fluid Machinery,2020,48(12):43-48+57.

[6] Ying Rui, Jiang Jin, Li Yanhui, et al. Flow field characteristics and particle classification Performance analysis of an Inner Cone Cyclone [J]. Journal of South China University of Technology (Natural Science Edition),20,48(04):95-103.

[7] Wei Kefeng, Zhao Qiang, Cui Xiaoliang, et al. Numerical Experimental study on Influence of Cone Angle on Flow Field and Separation Performance of Hydrocyclone [J]. Metal Mine, 2019 (04): 147-153.

[8] Jing Qi. Analysis on separation mechanism of gas-liquid cyclone separator [J]. Yunnan Chemical Industry, 2018, 45(10): 236-237. (in Chinese)

[9] Quan Hongbing, Zhang Yong, Zhang Guangyi, et al. Analysis of Flow Field and Spin-separation Efficiency of Hydrocyclone Based on CFD [J]. Chinese Internal Combustion Engine and Accessories,2018(02):208-211.

[10] Cheng Zhiliang, Qiu Facheng, Xu Fei, et al. Effect of separation space Structure on flow field and mass transfer Area of cyclone [J]. Chemical Engineering,2017,45(03):52-58+63. (in Chinese)

[11] Yang Fei, Qiu Shuang, Liu Yeqin. Research on the Internal Flow Field of a New Cyclone Based on fluent [J]. Chinese Internal Combustion Engine and Accessories,2017(12):45-47.

[12] Zhang Beibei, Jiang Minghu, Xing Lei, et al. Flow Field Analysis of a New Hydrocyclone with Different Inlet Velocity [J]. Journal of Daqing Normal University,2016,36(06):94-96.